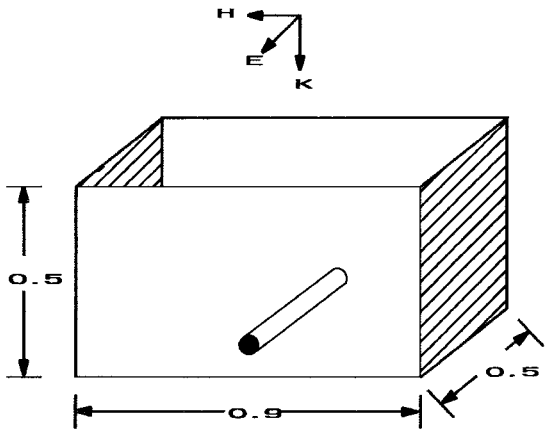

Fig. 2. Open box geometry. Dimensions in meters, hatched lines indicate open-circuit boundaries.

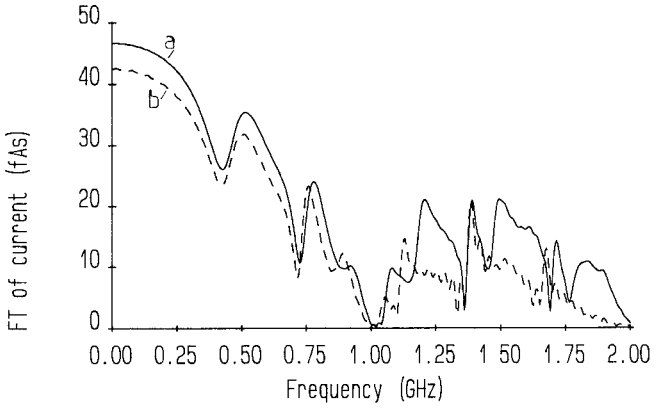

Fig. 3. Comparison of the frequency spectra for the geometry of Fig. 2 using *a*) fine mesh and *b*) wire node.

First, a fine mesh ($45\times25\times25$ nodes) model of this geometry was constructed using the ordinary symmetrical, condensed node, where the wire was modeled in the normal way by short-circuiting the transmission lines at a distance $\Delta l/2$ from the wire center. This is a slightly more accurate model than the short-circuit node mentioned in Section I and, for the problem under consideration, models an effective wire radius of 0.011 m.

Second, exactly the same problem was modeled using a coarse mesh of $9\times5\times5$ nodes. In this case a wire of radius 0.011 m cannot be described by short-circuiting nodes, as the nodal distance is too large ($\Delta l = 0.1$ m). For this reason, the thin wire was modeled using the new wire node. Substituting $r = 0.011$ m in (3) gives the admittance and hence the scattering matrix of the wire node.

Both numerical models of the problem were subjected to a plane wave impulse excitation as shown in Fig. 2. Results for the wire current obtained from the two models are compared in Fig. 3 (frequency response) and Fig. 4 (impulse response). Solid lines are for the conventional model using fine mesh and short-circuited nodes to model the wire. Broken lines are for the coarse mesh and the new wire node modeling the wire. Considering the differences in the modeling approach in the two cases, the agreement is excellent up to 1 GHz. This suggests that the wire node can accurately model thin wires ($r \ll \Delta l$). Agreement above approximately 1 GHz is less good, but this is not due to the properties of the wire node. It is due to a general deterioration in

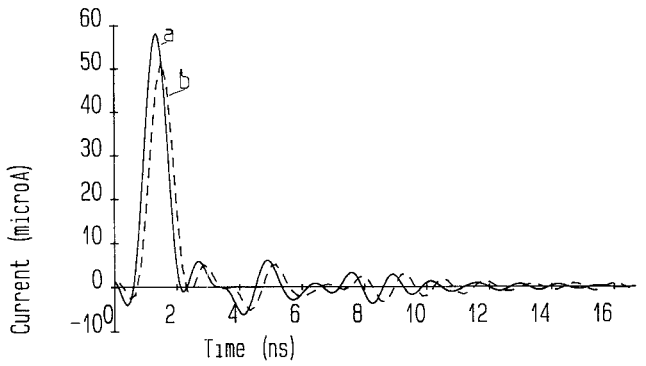

Fig. 4. Comparison of the time-domain response for the geometry of Fig. 2 Filtered to 1 GHz using *a*) fine mesh and *b*) wire node.

accuracy in modeling the field problem, as the number of nodes per wavelength is too small above this frequency.

The use of the wire node results in enormous benefits. For the example given, there is a 1/625 saving in computer execution time and a 1/125 saving in storage with little loss in accuracy.

At present only wires at the center of the node have been modeled. It should be possible in the future, using this technique, to model thin wires, off-center and multiconductor wires provided the scattering matrix can be calculated.

The wire node marks an important development in TLM, as it makes possible the description of thin wires within a coarse mesh, thus offering substantial savings in computer storage and run time.

Work is in progress to study the behavior of the wire node in different configurations, especially near terminations.

ACKNOWLEDGMENT

The authors wish to acknowledge the contribution to this work made by the late Professor P. B. Johns.

REFERENCES

[1] P. B. Johns, "The art of modeling," *IEEE Electron and Power*, pp. 565–569, Aug. 1979.
[2] P. Naylor, C. Christopoulos, and P. B. Johns, "Coupling between electromagnetic field and wires using transmission-line modelling," *Proc. Inst Elec. Eng.*, vol. 134, pt A, no. 8, pp. 679–686, Sept. 1987.
[3] P. B. Johns, "New symmetrical condensed node for three-dimensional solution of electromagnetic-wave problems by TLM," *Electron Lett.*, vol. 22, no. 3, pp. 162–164, Jan 1986.
[4] P. B. Johns, "A symmetrical condensed node for the TLM method," *IEEE Trans. Microwave Theory Tech.*, vol. MTT-35, pp. 370–377, Apr 1987.
[5] R. E. Collin, *Foundations for Microwave Engineering*. New York: McGraw-Hill, 1966.

Anisotropic Measurements of Rubber Sheets with an *X*-Band Three-Wave Interferometer

RENÉ SARDOS, JEAN-FRANÇOIS ESCARMANT, AND EMMANUEL SAINT-CHRISTOPHE

***Abstract*—A three-wave recording interferometer has been modified in order to adapt it for the anisotropic measurements of rubber sheets**

Manuscript received April 4, 1989; October 23, 1989.
The authors are with the Laboratoire de Physique Expérimentale et des Microondes, Université de Bordeaux I, 351, Cours de la Libération, 33405 Talence, France.
IEEE Log Number 8933000.

containing carbon particles. Due to the modifications made, it is no longer necessary to use an anechoic chamber, and the disadvantages of antennas are eliminated, together with diffraction along the edges of samples. After a description of the experimental instrument, some of the measurement results are presented.

I. Introduction

Rubber sheets containing carbon particles have anisotropy which is due to their manufacturing process. Because of the considerable absorption quality of these sheets and the scattered nonhomogeneity of their materials (due to the polymer chains containing carbon particles [1]), cavity studies are not satisfactory and in general are not attempted. The study procedures generally used for these measurements utilize an anechoic chamber. The sample is placed some 10 m from an emitting antenna and the reflected signal is analyzed with a receiving antenna. The use of two antennas does not allow one to work along the orthogonal direction of the sheet. In addition, because of the diagrams of the antennas and the size of the sample one can risk obtaining (a) diffraction along the edges of the sample and (b) sample–antenna and antenna–antenna couplings. One of the most recent instruments proposed [1] functions in very brief pulses, which enables one to avoid certain shortcomings.

We have modified a three-wave interferometer created by Sardos [2] in order to adapt it for the anisotropic measurement of rubber sheets. These anisotropies are generally much greater than those obtained with paramagnetic salts or with semiconductors placed in a magnetic field [3]–[5]; there is thus no difficulty in measuring them.

II. Analysis Method

A three-wave interferometer, operated in X-band, was modified to work by reflection. In addition, a circulator and a rectangular-to-circular waveguide transition introduced before a TE_{11} rotary joint were inserted in order to turn the rubber sample around its axis.

In a two-wave interferometer, two beams issuing from the same source are allowed to interfere. With at least a part of the wave propagating in the waveguides, the signals that interfere can be shown to have the form

$$E_1 = A_1 \exp\left[j\left(\omega t - \varphi_1 - \frac{2\pi d_1}{\lambda_g} \right) \right]$$

and

$$E_2 = A_2 \exp\left[j\left(\omega t - \varphi_2 - \frac{2\pi d_2}{\lambda_g} \right) \right].$$

The signal resulting from the addition of these two vibrations has the value

$$E = E_1 + E_2.$$

Detection being generally quadratic, one looks for the square of the amplitude of this vibration ($E \cdot E^*$):

$$I = A_1^2 + A_2^2 + 2A_1A_2 \cos\left(\varphi_2 - \varphi_1 - 2\pi \frac{d_1 - d_2}{\lambda_g} \right).$$

To obtain maximum sensitivity, one usually searches for a null by adjusting the phase shifters and attenuators. A null is obtained when $A_1 = A_2$ and

$$\varphi_2 - \varphi_1 - 2\pi \frac{d_1 - d_2}{\lambda_g} = (2k+1)\pi.$$

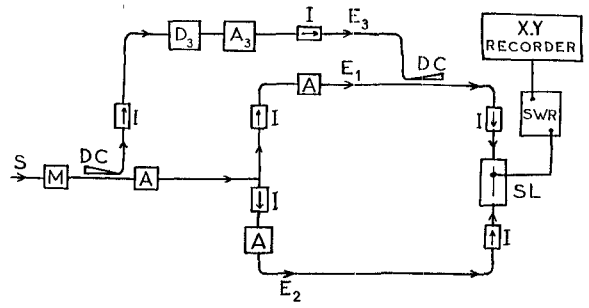

Fig. 1. The three-wave interferometer. S—source; M—modulator; I—isolator, A—attenuator; D—phase shifter; DC—directional coupler; SL—slotted line; SWR—amplifier.

Measurement is made in two stages; a null is first obtained in the absence of the phenomenon to be studied, then in the presence of the phenomenon.

Let us now consider the case of a three-wave interferometer (Fig. 1). The waves

$$E_1 = A_1 \exp\left[j\left(\omega t - \varphi_1 - 2\pi \frac{d_1}{\lambda_g} \right) \right]$$

$$E_2 = A_2 \exp\left[j\left(\omega t - \varphi_2 - 2\pi \frac{d_2}{\lambda_g} \right) \right]$$

$$E_3 = A_3 \exp\left[j\left(\omega t - \varphi_3 - 2\pi \frac{d_3}{\lambda_g} \right) \right]$$

are arranged to interfere in a slotted line which serves as both a mixer and a phase shifter. One obtains a voltage

$$E' = E_1 + E_2 + E_3$$

the square of which has the value

$$I' = A_1^2 + A_2^2 + A_3^2 + 2A_1A_2 \cos\left(\varphi_2 - \varphi_1 - 2\pi \frac{d_1 - d_2}{\lambda_g} \right) + 2A_1A_3 \cos\left(\varphi_1 - \varphi_3 - 2\pi \frac{d_3 - d_1}{\lambda_g} \right) + 2A_2A_3 \cos\left(\varphi_2 - \varphi_3 - 2\pi \frac{d_3 - d_2}{\lambda_g} \right).$$

In our case, the phenomenon to be studied will be in arm 2. Thus waves E_1 and E_3 will not vary during the course of the study; only wave E_2 will vary in phase and in amplitude. As a consequence

$$dA_1 = d\varphi_1 = dA_3 = d\varphi_3 = 0.$$

Let us assume that

$$A_3 = \frac{A_1}{n} \quad \text{and} \quad \varphi_3 = \varphi_1 - 2\pi \frac{d_3 - d_1}{\lambda_g} - \gamma.$$

The differential of I' has the value

$$d(I') = 2A_2\,dA_2 + 2A_1\,dA_2 \cos\left(\varphi_2 - \varphi_1 - 2\pi \frac{d_1 - d_2}{\lambda_g} \right) - 2A_1A_2 \sin\left(\varphi_2 - \varphi_1 - 2\pi \frac{d_1 - d_2}{\lambda_g} \right) d\varphi_2 + 2\frac{A_1}{n}\,dA_2 \cos\left(\varphi_2 - \varphi_1 - 2\pi \frac{d_1 - d_2}{\lambda_g} + \gamma \right) - 2A_2 \frac{A_1}{n} \sin\left(\varphi_2 - \varphi_1 - 2\pi \frac{d_1 - d_2}{\lambda_g} + \gamma \right) d\varphi_2.$$

TABLE I

γ	0	$\pi/2$	π	$3\pi/2$
$d(I')$	$-\frac{2A_1}{n}dA_2$	$\frac{2A_1^2}{n}d\varphi_2$	$\frac{2A_1}{n}dA_2$	$-\frac{2A_1^2}{n}d\varphi_2$

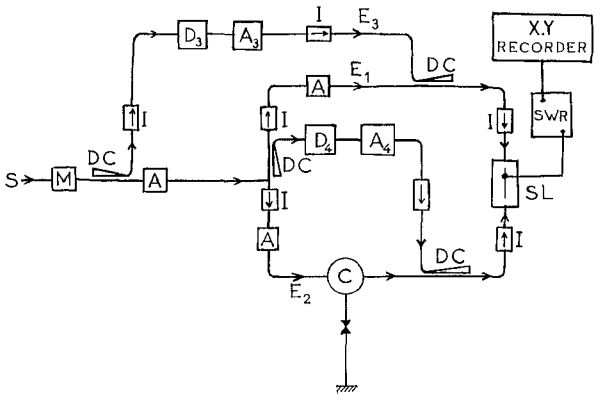

Fig 2 Modified three-wave interferometer. C—circulator; other letters identified in Fig 1.

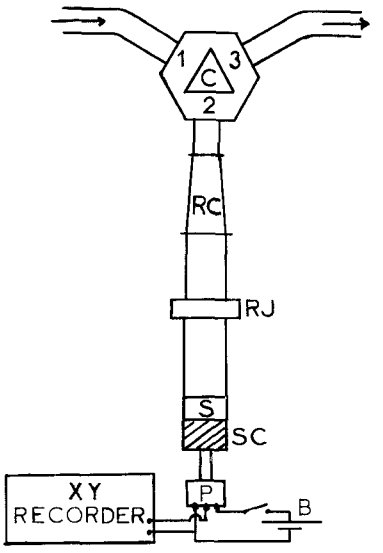

Fig. 3. RC—rectangular-to-circular transition; RJ—rotating joint; S—sample; SC—short-circuit; P—potentiometer; B—battery.

Let us suppose that the instrument is adjusted before the variation of wave E_2 so that $A_1 = A_2$ and consider the position where

$$\varphi_2 - \varphi_1 - 2\pi\frac{d_1 - d_2}{\lambda_g} = (2k+1)\pi$$

that is, the position necessary to obtain a null when a two-wave interferometer is being used (one renders $A_3 = 0$ with an attenuator, $n = \infty$, in order to establish the necessary condition). When E_2 varies upon inserting the sample, one will have

$$d(I') = -\frac{2A_1}{n}dA_2\cos\gamma + 2\frac{A_1^2}{n}d\varphi_2\sin\gamma.$$

For the special values of γ, Table I gives the corresponding values of $d(I')$.

Thus, if wave 3 is in phase or in phase opposition with wave 1, one obtains a variation of intensity dependent on the variation of amplitude, dA_2, but independent of the variation of phase, $d\varphi_2$. One can thus measure dA_2 and record it in relation to an exterior variable (magnetic field, for example) acting on a sample placed in arm 2.

When, on the other hand, wave 3 is in early or late phase quadrature with wave 1, the variation of intensity is independent of the variation of amplitude dA_2 and depends only on the variation of phase $d\varphi_2$, which we can consequently measure.

The three-wave interferometer thus enables one, with this particular adjustment, to measure separately the weak phase and amplitude variations and to conduct their uninterrupted recording. It can be shown that, when the variations of wave 2 are greater, that is, when they are ΔA_2 and $\Delta\varphi_2$, the higher order terms that appear eliminate one another with the average of the results obtained (for $\gamma = 0$ and $\gamma = \pi$ and for $\gamma = \pi/2$ and $\gamma = 3\pi/2$); one thus obtains ΔA_2 and $\Delta\varphi_2$. The instrument enables one to measure values $\Delta A_2/A_2 \geqslant 2.5\cdot 10^{-5}$ and $\Delta\varphi_2 \geqslant 5''$.

The apparatus shown in Fig. 1 had to be modified in order to adapt it for the study of the birefringence of rubber sheets containing carbon particles. To achieve this, a circulator (Fig. 2) was placed in arm 2. This circulator is followed by a rectangular-to-circular transition (containing a polarization sheet) long enough to have a reduced $VSWR$: 1.015). The TE_{01} mode of the rectangular guide is transformed into the TE_{11} mode of the circular guide. This transition is followed by a rotary joint for circular guide TE_{11} in order to make the sample, which was fitted into a circular guide 24.75 mm in diameter, turn. The rubber sheet fills up the whole section of the circular guide and is followed by a short circuit (Fig. 3).

This short circuit and the waveguide sample holder are connected with a helicoidal potentiometer in which a current flows. The voltage that appears is proportional to the angle and is applied to terminal X of an X,Y recorder. The values of $d(I')$ for $\gamma = 0$, $\pi/2$, π, and $3\pi/2$ can thus be recorded in relation to the angle. Such is the principle of the instrument.

III. Operation

The operation of this instrument poses a certain number of difficulties, some of them having been encountered during the initial linking up. For example, the isolators must be carefully tuned, especially in the "forbidden" direction, and the attenuators and phase shifters must be of the rotating type. Other difficulties appeared because circulators are never perfect and their scattering matrices never correspond to the theoretical matrix, which is

$$[S] = \begin{bmatrix} 0 & 0 & 1 \\ 1 & 0 & 0 \\ 0 & 1 & 0 \end{bmatrix}.$$

In our use, certain nonzero terms are more troublesome than others. We will thus begin with the general matrix to make the analysis of the influence of small but nonzero coefficients:

$$\text{General matrix } [S] = \begin{bmatrix} S_{11} & S_{12} & S_{13} \\ S_{21} & S_{22} & S_{23} \\ S_{31} & S_{32} & S_{33} \end{bmatrix}.$$

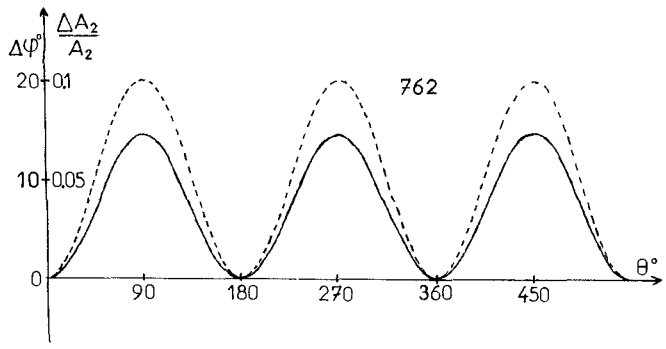

Fig. 4. Value of $\Delta A_2/A_2$ (solid line) and $\Delta\varphi_2$ (dotted line), for 762 sheets, versus angle θ.

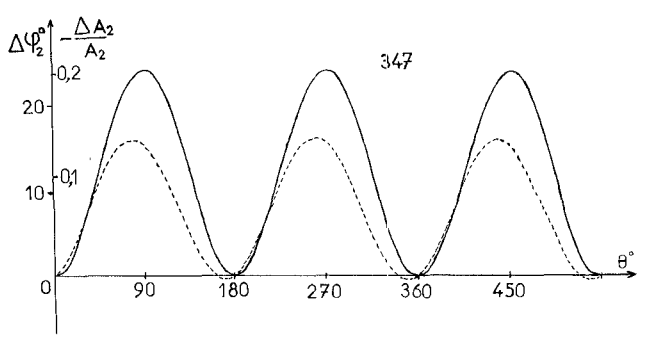

Fig. 5. Value of $\Delta A_2/A_2$ (solid line) and $\Delta\varphi_2$ (dotted line), for 347 sheets, versus angle θ

Our purpose is to have the wave entering arm 1 of the circulator go into arm 2. This wave (Fig. 3) then propagates to the rubber sample. A part reflects on the front side, the other part penetrates into the sheet and flows towards the short circuit while weakening. A part reflects on it again, the other crosses the front side, etc. In short, one has multiple reflections in the sheet, and the resulting wave E_2 returns to the circulator (arm 2). At this point it is important that the wave does not reflect and return to the sample; thus S_{22} should be as small as possible (were this not the case, one would have multiple reflections, versus distance, between the circulator and the sample). One is thus obliged to make a special adjustment of arm 2 of the circulator (one obtains a *VSWR* of 1.015).

The wave that comes into arm 1 of the circulator does not enter entirely into arm 2; a part goes directly into arm 3, for S_{31} is not absolutely zero. This wave is particularly bothersome because it interferes in the slotted line with the wave that was reflected from the sample and produces an error. In order to reduce S_{31} to a zero value, we have employed a subterfuge: wave E_4 (Fig. 2), which has an amplitude equal to the wave entering directly into arm 3 and a phase opposite to it, is injected. One thus artificially renders S_{31} of the whole equal to zero. This result is obtained by placing (after having made the adjustment of arm 2) in arm 2 of the circulator a movable termination of excellent quality ($VSWR = 1.005$) and by placing in arm 3, behind the coupler bringing wave E_4, a very carefully adjusted detector. Theoretically the result is obtained when, after having regulated the phase shifter and attenuator of arm E_4, a minimum zero is obtained in the detector regardless of the position of the movable termination of arm 2.

Thus modified, the instrument can measure values $\Delta A_2/A_2 = 10^{-4}$ and $\Delta\Phi_2 = 1'$ versus θ. The decrease in precision is due mainly to the rotary joint.

IV. Measurements

For an ellipse a variation $\Delta A_2/A_2 = 10^{-4}$ corresponds to $b = a(1-10^{-4})$, that is, to $\beta = b/a = 0.9999$. Very weak anisotropies can thus be measured.

With the instrument connected and regulated, we proceeded to make measurements concerning the synthetic elastomer S.B.R. containing, in one case, black no. 347, and, in the other, black no. 762, both 37.5 percent by weight.

The zero of the interferometer was obtained in each case when the rolling direction of the sheet was parallel to vector $\boldsymbol{E}$ of the wave. Fig. 4 refers to the S.B.R. sample containing black no. 762. One sees that the curves are sinusoidal and that their maxima and minima correspond respectively to the same value of the angle of rotation θ.

Measurement of the reflection coefficient of the sample followed by a short circuit gives $R(0)$ and $\varphi(0)$ when $\theta = 0$. Using these values, and the values of the reflection coefficient of the short circuit, we can then determine $\epsilon'(0)$ and $\epsilon''(0)$. For a different θ, one obtains, taking into consideration the fact that $\Delta R = \Delta A_2$ and $R = A_2$, $R(\theta) = R(0) + \Delta R(\theta)$ and $\varphi(\theta) = \varphi(0) + \Delta\varphi(\theta)$, and the calculation then produces $\epsilon'(\theta)$ and $\epsilon''(\theta)$.

Fig. 5 gives the result obtained for S.B.R. containing black 347 at 37.5 percent by weight. The phenomena are of different amplitudes; the sign of $\Delta A_2/A_2$ is reversed in relation to the preceding but the minima and maxima do not coincide exactly—there is a shift of $10 \pm 1°$.

V. Conclusion

The instrument, which is conceived to measure anisotropies in a very general manner, is adapted easily for the special case of elastomers containing carbon black. An anechoic chamber is not necessary and there are no problems with antennas or the coupling of antennas, which are simply not required. In addition, only relatively small samples are necessary. The results obtained for an elastomer containing two types of carbon black highlight the differences in anisotropies as well as the shift between the two curves obtained in the case of black 347. An analogous phenomenon, but on a larger scale, has already been pointed out by Hashimoto and Shimizu [1], who attributed it to the type of black used.

Acknowledgment

The authors would like to thank Manufacture Française des Pneumatiques Michelin (Clermont-Ferrand, France) for kindly supplying them with samples of rubber sheets.

References

[1] O. Hashimoto and Y. Shimizu, "Reflecting characteristics of anisotropic rubber sheets and measurements of complex permittivity tensor," *IEEE Trans. Microwave Theory Tech.*, vol MTT-34, pp. 1202–1207, Nov. 1986.

[2] R. Sardos, "Etude et réalisation d'un interféromètre hertzien à trois ondes de grande sensibilité," *Rev. Phys. Appl.*, vol. 4, pp. 29–32, 1969.

[3] J. Royaud and R. Sardos, "Etude en bande *X*, à basse température, des raies d'absorption $\Delta M = \pm 3$ et $\Delta M = \pm 2$ de quelques substances paramagnétiques," in *Proc. XIVth Congress Ampere* (Heidelberg-Geneva) 1976, pp 537.

[4] R Chastanet, Thèse Doc. Sc Phys. Bordeaux I, 1982

[5] K. Haye and R. Sardos, "Mise en évidence de divers effets magnéto-électriques dans une lame de Silicium n emplissant complètement la section d'un guide rectangulaire bande X," *Physica B* 154, pp. 344–352, 1989.

[6] A. R. Von Hippel, *Dielectric Materials and Applications*. New York: Wiley, 1958.